BIOCHEMISTRY
including biophysical chemistry & molecular biology
Article

Biochemistry **2010,** *49,* 8831–8838 8831
DOI: 10.1021/bi1008936

Kinetic Studies of the Interaction of β-Lactoglobulin with Model Membranes: Stopped-Flow CD and Fluorescence Studies

Ning Ge, Xiuqi Zhang, and Timothy A. Keiderling*

Department of Chemistry, University of Illinois at Chicago, 845 West Taylor Street (m/c 111), Chicago, Illinois 60607-7061

Received June 2, 2010; Revised Manuscript Received September 3, 2010

ABSTRACT: β-Lactoglobulin (βLG) is a member of the lipocalin protein family and has been shown to undergo changes in structure upon interaction with various surfactants and lipid vesicles. Dynamic light scattering (DLS) and Fourier transform infrared (FTIR) were used to study the interaction of dimyristoylphosphatidylglycerol (DMPG) vesicles with βLG and showed that the vesicles increase in size and become more dispersed and the transitions become broader but the lipid IR spectra and transition temperatures are stable. Fluorescence studies with vesicles with trapped calcein demonstrate βLG binding induces leakage in DMPG vesicles. To study the dynamics of the interaction between βLG and lipid vesicles further, we undertook kinetic studies using stopped-flow methods. Following previous equilibrium studies, three lipids, DMPG, dioleoylphosphatidylglycerol, and distearoylphosphatidylglycerol, all having the same negatively charged headgroup but with different acyl chain lengths, were used to prepare vesicles. Kinetic circular dichroism and fluorescence decays were measured simultaneously to monitor changes in secondary and tertiary structures, respectively. These were fit to either single- or double-exponential functions, and a multistep model, with at least two intermediate states, has been proposed to explain the major states seen in the kinetic interaction of βLG with lipid vesicles.

Interaction between proteins and membranes has long been an important aspect in understanding protein folding and misfolding. The genome encodes a great number of membrane-bound or active proteins. Furthermore, many extracellular proteins interact with membranes and/or membrane proteins as part of their function. This is particularly important for signaling and transport processes. Inclusion of membrane and/or membrane models in experimental studies can complicate data analysis and inhibit use of atomistic methods like crystallography or nuclear magnetic resonance (NMR).[1] However, optical spectral methods can be applied to such complex systems and yield useful, even if global or averaged, structural data. Optical spectra also have the advantage of a very fast time response for following the dynamics of structural changes.

β-Lactoglobulin (βLG), an 18300 kDa protein found in mammalian milk, is a member of the lipocalin protein family and has been shown to interact with various surfactants and lipid vesicles (*1*). However, its biological function is not clear (*2*). In its native state, βLG adopts a flattened β-barrel structure composed of a short α-helix and eight β-strands that form a hydrophobic core that can provide a binding site for fatty acids and other nonpolar molecules (*3*). A ninth β-strand is used to form a dimer at physiological pH, which dissociates into the monomer form below pH ∼2 (*4*−*6*). Although the βLG secondary structure is mainly that of a β-sheet protein in its native state, structure prediction algorithms suggest that various segments of its sequence have a strong propensity to adopt helical structures (*7*). Equilibrium studies have shown that βLG undergoes a β-sheet to α-helix transition in the presence of alcohol (*7*, *8*) and ionic surfactants (*9*, *10*). In addition, kinetic studies have shown that βLG goes through an α-helical intermediate form when it refolds from a denatured, disordered form (random coil) (*11*−*13*). Our lipid interaction studies have shown that anionic vesicles can also induce such a β-to-α conformational change in βLG (*14*, *15*). The interaction between βLG and lipid vesicles is concentration-dependent, and its strengths and mechanism vary with pH (*14*). Electrostatic interaction is a prerequisite to this conformational change, while hydrophobic interaction between exposed nonpolar residues and the lipid bilayer plays a role in stabilizing helices that develop from this sequence. The extent of penetration of βLG into the lipid vesicles also relates to characteristics of the lipids used, their packing, and the pH (*15*).

In this study, we address the kinetic aspects of this lipid-driven conformational change to further understand dynamic processes and any intermediate phases that could be exposed by varying the driving forces using different lipid vesicles. To satisfy the requirement of electrostatic interaction that appears to be a prerequisite for βLG−lipid vesicle interaction, we have used three lipids that have the same headgroups but vary in the lengths and character of their lipid acyl chains. This in turn serves to modify the lipid bilayer stability and its potential for hydrophobic interaction with the bound protein. In the kinetic experiments, stopped-flow CD and fluorescence were used to monitor changes in the secondary and tertiary structure, respectively, of the protein upon binding to the lipid vesicles. For fluorescence detection, the two Trp residues provide the probe, which can be additionally modified by lipid−protein interaction.

*To whom correspondence should be addressed. E-mail: tak@uic.edu. Telephone: (312) 996-3156. Fax: (312) 996-0431.

[1]Abbreviations: CD, circular dichroism; FTIR, Fourier transform infrared; βLG, β-lactoglobulin; DMPG, dimyristoylphosphatidylglycerol; DSPG, distearoylphosphatidylglycerol; DOPG, dioleoylphosphatidylglycerol; SUVs, small unilamellar vesicles; MLV, multilamellar liposome suspension; LUVs, large unilamellar vesicles; DLS, dynamic light scattering; NMR, nuclear magnetic resonance.

Published on Web 09/07/2010

Because our previous work focused on equilibrium studies of the interaction between βLG and lipid vesicles (*14*, *15*), those conclusions are noted briefly and extended here with new results for the purpose of background illustration. The additional data presented here develop rate constants for various kinetic phases and result in a proposed mechanistic pathway in the process. In addition, perturbation of lipid vesicles by βLG binding was studied by FTIR temperature and fluorescence leakage measurements, which may suggest possible functions for βLG.

MATERIALS AND METHODS

Materials. Bovine βLG, crystallized and lyophilized three times, was purchased from Sigma (St. Louis, MO) and used without further purification. Dimyristoylphosphatidylglycerol (DMPG), distearoylphosphatidylglycerol (DSPG), and dioleoylphosphatidylglycerol (DOPG) were obtained from Avanti Polar Lipids, Inc. (Alabaster, AL). Other chemicals were purchased from Sigma.

Preparation of Lipid Vesicles. Fresh small unilamellar vesicles (SUVs) were prepared just before being used by sonication of larger multilamellar vesicles using literature techniques (*14*). Briefly, the required amount of lipid was dissolved in chloroform or a chloroform/methanol mixture (3:1, v/v) at various concentrations, and the resulting lipid solutions were dried under a mild stream of N_2 while being shaken gently to form a thin film on the vial wall. The film was then hydrated via addition of the desired buffer [typically 20 mM phosphate buffer (pH 6.8 or 4.6)] and vortexed extensively. The resulting multilamellar liposome suspension (MLV) was then immersed in a bath sonicator (Branson 2200, Bransonic) for approximately 30−60 min, until the MLVs were dispersed into a clear suspension of SUVs. DLS measurements (see below) showed these to have relatively large distributions with radii typically dependent on preparation methods. Our goal was to obtain a clear, low-scattering, solution for CD and fluorescence measurements so that the actual size of the SUVs was not a prime criterion. The βLG stock solution was then slowly added to the aqueous lipid vesicle solution. This solution was mixed well and allowed to equilibrate prior to the study of the protein−lipid complex formed. We have found that after 1 h the CD and fluorescence intensities do not change further, indicating attainment of an equilibrated protein−lipid binding.

Fresh large unilamellar vesicles (LUVs) were prepared using an extrusion method. The required amount of lipid was dissolved in chloroform or a chloroform/methanol mixture (3:1, v/v), and the resulting lipid solutions (typically 3 mM) were dried under a mild stream of N_2 while being shaken gently to form a thin film. The film was then hydrated via addition of buffer [typically 20 mM Tris-HCl buffer and 10 mM NaCl (pH 7.0) or 20 mM phosphate buffer] and then vortexed extensively to form multilamellar vesicles (MLVs) (*16*−*18*). The MLVs were then reduced to uniform LUVs when the suspension was passed 15 times through a polycarbonate membrane with a mean pore diameter of 100 nm using an extruder (Avestin Inc., Ottawa, ON). These had a narrower size distribution (by DLS) with a maximal radius of ~65 nm.

CD Measurements. Far-UV CD spectra were recorded under equilibrium conditions on a J-810 spectrometer (Jasco, Easton, MD) using quartz cells with path lengths of 1 mm for protein concentrations of 0.2 mg/mL. An average of eight scans at 50 nm/min acquired with a bandwidth of 0.2 nm and a response time of 1 s were accumulated. The final spectra were obtained via subtraction of a background spectrum obtained under the same conditions with just buffer or for vesicles without protein placed in the same cell.

Fluorescence Measurements. Equilibrium fluorescence measurements were recorded from 300 to 450 nm on a Fluoromax-3 spectrofluorimeter (Jobin-Yvon Inc., Edison, NJ) for samples containing 0.2 mg/mL βLG held in a 1 mm path length cuvette, using an excitation wavelength of 295 nm. In all experiments, background spectra, either for the buffer alone or for the buffer containing only vesicles, were subtracted from the corresponding sample spectra.

FTIR Measurements. Sample solutions of βLG and DMPG at 3 mg/mL and 27 mM, respectively, in deuterated phosphate buffer (pH 7.0) were used for FTIR and measured as previously described (*14*, *15*, *19*, *20*). The samples were transferred to a homemade demountable cell composed of two CaF_2 windows separated by a 100 μm Teflon spacer clamped together in a brass holder. The FTIR spectra were recorded on a FTS60A spectrometer (Digilab, Randolph, MA) using a nominal resolution of 4 cm^{-1} by averaging 1024 scans with a zero-filling factor of 8. Temperature-variation experiments were conducted when the sample was placed in a homemade cell holder controlled from 5 to 60 °C in steps of 5 °C by flow from a bath (Neslab RTE 111) as previously described (*21*, *22*).

Light Scattering Measurements. Vesicle diameter sizes were characterized using a DynaPro dynamic light scattering (DLS) apparatus (Wyatt Technology, Santa Barbara, CA), via autocorrelation of the 90° scattering intensity at 830 nm. The data were analyzed in terms of an effective diameter, d_{eff}, using the Stokes−Einstein equation:

$$d_{eff} = (k_B T)/(3\pi\eta D) \quad (1)$$

where k_B is the Boltzmann constant, T is the temperature (35 °C), η is the solvent viscosity, and D is the diffusivity from the first cumulant. The quantitative d_{eff} values obtained were sensitive to the analysis parameters chosen, but the trends were reproducible with sufficient care in sample preparation; only general observations are reported here.

Calcein Leakage Measurements. LUVs were also prepared as described above using Tris buffer containing 100 mM calcein, and untrapped calcein was removed by gel-filtration chromatography using a Sephadex G-50 column (length of 25 cm, diameter of 1.0 cm). The concentration of liposome was measured by the phosphorus analysis method (~0.3−0.4 mM) (*23*). In a concentrated environment, inside the vesicle, calcein emission is quenched, but if the vesicle leaks, the dilute calcein has increased fluorescence. Calcein fluorescence was measured using excitation and emission detection wavelengths of 490 and 520 nm, respectively, starting ~1 h after addition of βLG to a calcein-containing liposome, to obtain an equilibrium interaction. Calibration of the range of vesicle leakage was obtained by using fluorescence from vesicles with no βLG as the 0% leakage standard and that from liposomes dispersed with 10% Triton X-100 as the 100% standard (*24*).

Stopped-Flow Measurements. An SFM-400 rapid mixer (Biologic) equipped for stopped-flow measurements with a SF-20 fluorescence cell was used for the kinetic experiments (*25*). The whole system was kept above the lipid transition temperature using flow from a temperature-controlled water bath. To obtain more excitation intensity at 225 nm, a 150 W Xe−Hg lamp was substituted in the stopped-flow experiment for the Xe lamp normally used for steady-state CD measurements. Variable controlled mixing

of the contents of two syringes containing SUVs and βLG was used to achieve final solutions with different lipid concentrations but the same βLG concentration via a change in the lipid:buffer mixing ratio. The CD signals versus time were recorded at 222 nm with a band-pass of 2 nm and a fixed HV optimized for the signal-to-noise ratio. The total fluorescence spectra beyond the cutoff were recorded at 90° to the excitation by use of a 320 nm long wave pass filter. For each experiment, 12−15 CD and fluorescence kinetic traces were collected simultaneously and separately averaged.

The final CD kinetic traces were obtained after subtraction of background traces that are the time-dependent signal obtained by mixing buffer with or without vesicles but without protein. We obtained the final fluorescence decays by dividing the total fluorescence as a function of time after mixing βLG with lipid by the similarly obtained kinetic trace for mixing of only βLG and buffer. The fluorescence normalization was done to compensate for photobleaching and other long-term behaviors indicated by a slight signal decrease with time for the mixing of βLG and buffer only. The time-dependent results were fit with multiple exponential functions to obtain kinetic parameters for various kinetic phases using Bio-Kin32 (Biologic).

RESULTS

Effect of βLG on Lipid Vesicles upon Interaction under Equilibrium Conditions. The transition temperature for ordering in the lipid bilayer in the vesicles was determined by monitoring the IR frequency for the CH_2 asymmetric and symmetric stretching modes of the aliphatic chains. As shown in Figure 1, for DMPG the frequency of the asymmetric CH_2 mode increases from 2919 to 2924 cm^{-1}, and that of the symmetric CH_2 mode increases from 2850.7 to 2853.7 cm^{-1}, as the temperature is increased from 5 to 60 °C. Mixing βLG with the vesicles results in little perturbation of the lipid structure; the spectra do not change, and the transition temperature for both modes stays at ~25 °C, which was determined by fitting the data with a sigmoidal thermodynamic model (*22*) (see Figure 1 and the fitted values in Table S1 for the temperature-dependent spectra shown in Figure S1, both in the Supporting Information). However, the transition does become broader, as is more evident for the symmetric mode, which could be consistent with an increased level of dispersion in vesicle size and the loss of bilayer wall integrity (see below). Parallel thermal transition tests with DOPG and DSPG were not undertaken because of their relatively inaccessible transition temperatures.

Effects of protein binding on vesicle size were measured using dynamic light scattering (DLS). The SUVs had a relatively large size dispersion, so that the effects of protein binding on size could not be measured well; however, our LUV preparations had a narrower distribution. The average size of LUVs was significantly affected by the addition of a constant concentration of βLG (0.2 mg/mL), which appeared to roughly double the radius, but the effect varied with lipid concentration (data listed in Table S2 of the Supporting Information). Under our measurement conditions, for samples at > 2 mM, the radius of the vesicles increased from ~70 to > 100 nm after addition of βLG. At > 4 mM lipid, the increase in vesicle size appeared to decrease with an increased vesicle concentration, which may be indicative of a change from vesicles being saturated with protein (low DMPG concentration) to being protein limited (high concentration).

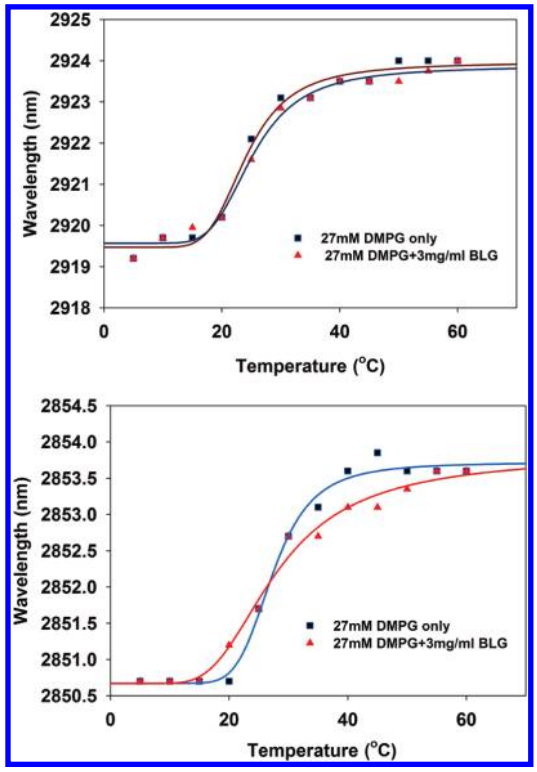

FIGURE 1: Temperature dependence of FTIR maxima for CH_2 stretching modes. The top panel shows the IR asymmetric stretching mode and the bottom panel the symmetric stretching mode. Black squares are frequencies for DMPG only; red triangles are frequencies for DMPG and βLG, and the blue and red lines are the best fits to these data with a sigmoidal thermodynamic model (*22*) (values in Table S1 of the Supporting Information).

Calcein leakage experiments to determine the effect of protein binding on membrane integrity were also conducted using LUV vesicles, which were chosen because of their ease of preparation with a trapped fluorescence dye. Calcein is quenched in the liposome interior if it is trapped at a high (100 mM) concentration and is not released from the liposome interior unless the lipid membranes are perturbed. If calcein leaks from inside the liposome, it becomes diluted in the outer aqueous phase of the liposome and its fluorescence yield increases. For these experiments, the vesicle amount was kept constant, but different amounts of βLG were added, thus varying the vesicle:βLG ratios. In Figure 2, it can be seen that as the DMPG:βLG ratio becomes lower, thus making more protein available to each vesicle, the degree of leakage increases. Our data indicate that βLG disrupts the vesicle wall integrity locally, leading to leakage by binding and insertion, and does not lyse the vesicle, because DLS indicated larger vesicles remain upon interaction. At these lipid:protein ratios, multiple protein interactions per vesicle are expected (*14*, *15*).

Stopped-Flow CD and Fluorescence Measurements. Time-dependent changes in the βLG structure occurring during the lipid−protein interaction were measured using stopped-flow kinetics simultaneously monitored with both far-UV CD and fluorescence detection. The α-helical content of βLG was monitored at 222 nm by far-UV CD and the tertiary structure change of βLG by the total fluorescence change (> 320 nm). Figures 3 and 4 show typical CD and fluorescence kinetic traces, respectively, following the time course of the protein−lipid interaction at pH 4.60 with different lipid:protein ratios while the concentration of protein was kept constant (0.2 mg/mL).

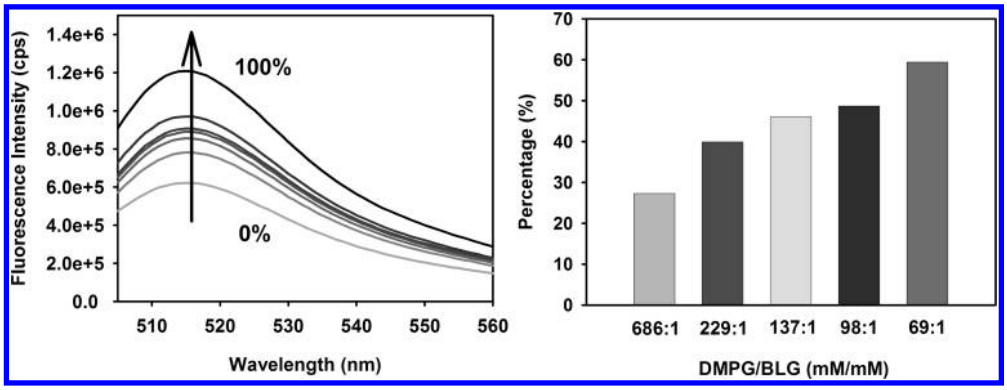

FIGURE 2: DMPG LUV leakage measurements. LUVs corresponding to ~0.3 mM DMPG were prepared loaded with 100 mM calcein; βLG was added to the LUVs, and the fluorescence was measured at 520 nm with excitation at 490 nm. The left panel shows the fluorescence measured with βLG added; 0% represents calcein-loaded LUVs only, and 100% denotes the spectrum in which all calcein is released from LUVs after addition of Triton X-100. The right panel shows a bar graph of the resultant percentage of leakage calculated for different DMPG:βLG ratios representing the five intermediate fluorescence curves on the left, which use the 0 and 100% values corresponding to the two marked extremal curves for calibration of the change.

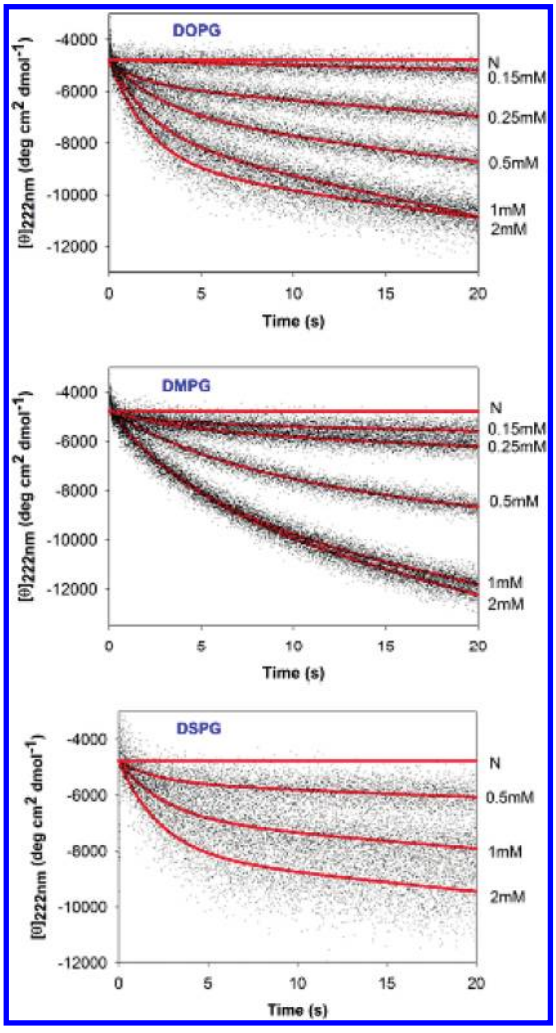

FIGURE 3: Stopped-flow CD kinetic traces for mixing of βLG and lipid SUV solutions in a 1:5 volume ratio to obtain final concentrations of 0.2 mg/mL for βLG and as labeled for the lipid. CD changes were measured at 222 nm. The value obtained for the mixing of βLG with buffer only is indicated by the trace labeled N and provides a baseline reference. Rate constants obtained are listed in Table 1.

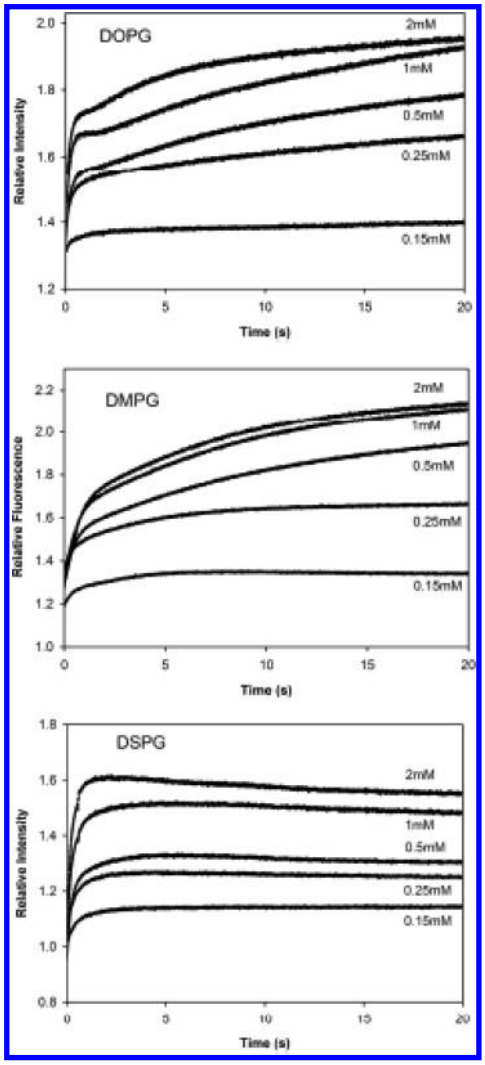

FIGURE 4: Stopped-flow total fluorescence (> 320 nm) kinetic traces for mixing of DMPG, DOPG, and DSPG with βLG at pH 4.60, as described for Figure 3 (simultaneous experiments). Solid lines are fits of the experimental data with double-exponential models; kinetic results are summarized in Table 2. The fit lines are normalized by dividing by the kinetic trace obtained from the mixing of βLG and buffer only.

Using an expected surface area per DMPG lipid molecule of ~0.6 nm^2 (*26*, *27*), a ratio of lipid to protein in the range of ~100−200:1, and a rough estimate of ~10 nm^2 for the βLG footprint, we expect there to be a substantial excess of vesicle surface for protein binding, and therefore, the kinetics should correspond to a pseudo-first-order process. Using a nonlinear

Table 1: Kinetic Rates and Amplitudes for the Mixing of βLG with Lipid Vesicles Monitored via CD

		rate constant k_1 (s^{-1})	amplitude (mdeg)
DOPG	0.15 mM	0.408 ± 0.032	0.851 ± 0.690
	0.25 mM	0.384 ± 0.047	3.753 ± 0.755
	0.5 mM	0.324 ± 0.021	7.241 ± 0.643
	1 mM	0.311 ± 0.088	10.140 ± 0.658
	2 mM	0.399 ± 0.042	14.369 ± 0.143
DMPG	0.15 mM	0.237 ± 0.023	2.000 ± 0.280
	0.25 mM	0.189 ± 0.020	3.237 ± 0.322
	0.5 mM	0.198 ± 0.011	7.514 ± 2.287
	1 mM	0.175 ± 0.027	13.601 ± 1.090
	2 mM	0.153 ± 0.032	15.501 ± 1.035
DSPG	0.15 mM	not available	not available
	0.25 mM	not available	not available
	0.5 mM	0.422 ± 0.041	4.329 ± 1.214
	1 mM	0.386 ± 0.001	7.776 ± 0.405
	2 mM	0.421 ± 0.009	12.645 ± 0.986

Table 2: Kinetic Rates for the Mixing of βLG with Lipid Vesicles Monitored via Fluorescence

		rate constant k_1 (s^{-1})	rate constant k_2 (s^{-1})
DOPG	0.15 mM	1.484 ± 0.304	not available
	0.25 mM	3.027 ± 0.093	0.123 ± 0.046
	0.5 mM	5.457 ± 0.375	0.091 ± 0.005
	1 mM	6.770 ± 0.654	0.068 ± 0.007
	2 mM	6.796 ± 0.254	0.134 ± 0.071
DMPG	0.15 mM	3.902 ± 1.556	0.253 ± 0.105
	0.25 mM	4.356 ± 0.612	0.222 ± 0.043
	0.5 mM	2.806 ± 0.251	0.124 ± 0.039
	1 mM	1.926 ± 0.215	0.121 ± 0.039
	2 mM	2.424 ± 0.681	0.116 ± 0.035
DSPG	0.15 mM	3.561 ± 0.465	0.729 ± 0.027
	0.25 mM	5.450 ± 0.010	1.032 ± 0.005
	0.5 mM	6.212 ± 0.118	0.795 ± 0.072
	1 mM	4.467 ± 0.583	0.737 ± 0.005
	2 mM	3.417 ± 0.014	not available

exponential regression method, each kinetic trace, $S(t)$, was fit by a sum of exponential terms, using the function

$$S(t) = at + b + \sum_i c_i \exp(-k_i t) \quad (2)$$

where k_i is the rate constant for the ith kinetic phase, c_i is the amplitude for the ith kinetic phase, and $at + b$ is a linear baseline that corrects for long-term drift in the signal due to bleaching and other instrumental problems (*25*). Each exponential term corresponds to one kinetic phase, and the coefficient indicates the fractional contribution to the overall transition of each kinetic phase. Rate constants found for the average of three trials of these kinetic experiments are listed in Tables 1 and 2, and the individual data for each, showing the distribution of values measured, are provided in Table S3 and S4 (Supporting Information).

The sample data traces in Figure 3 show changes in ellipticity at 222 nm after the mixing of βLG with DMPG, DOPG, or DSPG at various concentrations. Compared to the native state (labeled as solid line N), βLG gains negative ellipticity after being mixed with the lipid, and most of this change occurs after the mixing dead time (~6 ms). This CD change with time can be fit with a single-exponential curve, yielding rate constants for DMPG-induced βLG conformational change with values of ~0.2 s^{-1}, which were relatively independent of DMPG concentration, over this range (Table 1). The final amplitude achieved does increase with an increasing lipid concentration, paralleling the results found in our equilibrium studies (*14*, *15*). For the DOPG−βLG interaction, the rate constants for the CD change are roughly a factor of 2 faster, being between 0.3 and 0.5 s^{-1}, and also show no trend with DOPG concentration, but the amplitudes again increase, as expected. For the DSPG−βLG interaction, reliable rate constants cannot be obtained for low concentrations because of the small changes in ellipticity (small amplitudes) obtained, but at higher DSPG concentrations, rate constants of ~0.4 s^{-1} are measured, consistent with the trends seen in the CD kinetics for the other lipid vesicles. This lower amplitude in the dynamic behavior is consistent with our equilibrium results for DSPG obtained below the transition temperature, for which a smaller degree of βLG conformational transition was detected. In summary, the rate constants for (negative) ellipticity gain (corresponding to sheet-to-helix transition) caused by the interaction of βLG with a set of SUV vesicles, formed using different lipids having variable aliphatic chains, are comparable over the range of lipid concentrations studied.

Kinetic traces measured with fluorescence, monitoring results of tertiary structure changes, are more complex, as is shown in Figure 4. All fluorescence traces have been normalized by dividing by the corresponding trace for native-state βLG mixing with buffer, which corrects for some day-to-day variations due to the sample and instrument. All the curves show an initial increase in fluorescence as expected, which is faster ($k_1 \sim 2-6$ s^{-1}) than a slower further increase or decay ($k_2 \sim 0.1-1$ s^{-1}), and varied for different lipid systems. Beyond that, an increase in fluorescence during the dead time (burst phase) is also apparent in Figure 4, which might have been expected from earlier results with surfactants (see Discussion) (*33*). The fluorescence emission signal mainly comes from Trp19, located in the hydrophobic core, which was proposed following the observation that a W19A mutant had dramatically reduced (80%) fluorescence (*28*). The fluorescence of Trp61, on the surface of the protein, is generally assumed to be quenched by the adjacent Cys66−Cys160 disulfide bond. When βLG binds to the vesicle, its fluorescence shifts from ~336 to 332 nm and increases in intensity (>40%) (*14*). The increased fluorescence on membrane binding presumably indicates less quenching of Trp61 that accompanies formation of an altered (less compact) tertiary structure but one that shields both Trp residues from solvation.

For the DMPG−βLG interaction, all the traces for different lipid concentrations can be fit to a double-exponential curve (results summarized in Table 2). The primary rate constant (k_1) decreases somewhat with an increase in DMPG concentration but becomes steady above 0.5 mM. The secondary rate constants (k_2) also decrease with an increase in DMPG concentration and are slightly smaller than the CD rate constants, but are more reduced for higher DMPG concentrations. For the DOPG−βLG interaction, the fluorescence trace can be best fit to a single-exponential curve for low DOPG concentrations (0.15 mM) and fits better to a double-exponential curve for higher DOPG concentrations. The faster of the two rate constants (k_1) increases for increased DOPG concentrations but becomes steady above 0.5 mM. Although the slower rate constants (k_2) fluctuate with varying experimental conditions, they are again slower than the CD rate constants. For the DSPG−βLG interaction, the curves can also be fit to double-exponential phases and have fluctuating primary rate constants (k_1) with an increase in DSPG concentration.

However, the slower fluorescence rate constants, where comparable, are somewhat larger than the corresponding CD rate constants, which may due to the gel state of DSPG at these temperatures, while by contrast, DOPG and DMPG were both in liquid crystal states (above T_m).

DISCUSSION

FTIR spectroscopy can be used to study transitions in both protein secondary structure and DMPG vesicle structure (*29*). With an increase in temperature, the lipid alkyl chains have more flexibility, as indicated by the increase in the frequency of both CH_2 asymmetric and symmetric modes (*29*). As seen from the transition curves (Figure 1), binding of βLG to lipid vesicles does not significantly disturb the lipid transition equilibria, yielding the same T_m values but a somewhat broader transition. Combined with our previous results, although βLG inserts into the hydrophobic area of the lipid bilayer (*15*), it does not seem to affect the global organization or ordering of the vesicle. Interaction with βLG does cause an apparent increase in the size of the protein−vesicle complex, as indicated by light scattering measurement on LUVs with added βLG. Furthermore, upon binding to βLG, vesicles leak, as monitored by the loss of calcein from inside to outside the vesicle. These data suggest βLG may disturb the integrity of vesicle walls, but not their overall order or alkyl chain conformation.

Native-state βLG is a largely β-sheet protein with an amino acid sequence that when analyzed by secondary structure prediction algorithms indicates a strong potential for helical structure (*30*). Previous refolding kinetic studies indicate the presence of a transient intermediate, α-helical in nature, that accumulates within the mixing time of stopped-flow CD measurements (*11*,*31*,*32*). The transient CD data suggest the α-helical intermediate is characterized by an overshoot behavior, in which the ellipticity at 222 nm is greater than that for native βLG. These results suggest a case of nonhierarchical protein folding in which protein structures form early folding intermediates for which local interactions dominate. These presumably reduce the configurational space and stabilize the structure, allowing it to refold in response to nonlocal interactions balanced with the local ones. Kinetic studies of βLG interacting with surfactants such as DTAC also show βLG follows a β-to-α transition through an unfolding route in which an intermediate with mostly native secondary structure but loose tertiary structure appears between the native and α-states.

Because the lipids are in substantial excess relative to the protein in our experiments, pesudo-first-order processes are expected and the protein concentration should not affect unfolding rates. This is presumably the source of the roughly constant rates with the change in lipid concentration, the larger variation coming with a change in lipid and thus vesicle stability. There is a burst phase in the fluorescence decay within the mixing deadtime, as indicated by the initial normalized values in Figure 4 being higher than 1.0, which would be the value obtained for the decay of βLG only (no lipid). (There is also a 1−2 ms spike, not shown and not included in our data analyses, presumably caused by the initial mixing turbulence.) The previously reported kinetic study with DTAC micelles suggests that the burst phase may due to an initial process of dissociation of the dimer to monomer before unfolding, and our data would be consistent with such a model; however, we cannot test it without further development (*33*). In principle, one could design mutants to test the breakup kinetics of the dimer interface separately from the unfolding of the monomer. The previous surfactant studies have shown that βLG has a higher fluorescence intensity at acidic pH, at which βLG is a monomer, than neutral pH, at which βLG is in a dimer form. Our kinetic results show that the βLG β-to-α transition mechanism follows a path in which there is an intermediate with mostly native secondary and loose tertiary structure. This is indicated by the contrast between the biexponential fluorescence and the single-exponential CD decay found in our fits to the stopflow data. The faster rate constant found with fluorescence indicates a kinetic phase corresponding to a modification of tertiary (or like) structure resulting in a Trp environment change that precedes the kinetic phase indicated by CD decay. This may be preceded by an even faster breakup of the dimer structure in the burst phase. The CD decay indicates the change in secondary structure and helix formation follows a kinetic phase that is similar in rate to the slower phase found with fluorescence but in our hands is not the same. In particular, as the nature of the lipids is varied, the kinetic response of the slow step of fluorescence is different from that of the change in the CD under the same conditions, which implies that two separate processes of similar kinetics contribute to this slower step.

The concentrations of lipid vesicles used in this paper vary over a small range (0.15−2 mM), which may not be sufficient to unequivocally derive a pattern for how rate constants (faster fluorescence constant) depend on lipid vesicle concentration. The faster fluorescence rate constants cover only a small range, and the changes seen in our experiments may also be affected by error; thus, one should take caution in interpreting their detailed variations. The CD and the slower fluorescence rate constants do not vary significantly with lipid concentration, which suggests they correspond to a process that occurs after βLG binds to the vesicle. Such processes would then depend on βLG's intrinsic properties once βLG interacts with the charged vesicle surface and loses the constraints of its native tertiary structure, which presumably stabilizes the β-sheet fold. Thus, after disruption of the tertiary structure, βLG would have the opportunity to refold, reflecting the propensity of its primary sequence. This folding would be independent of lipid vesicle concentration, as long as there is enough lipid to destabilize the tertiary fold, and also could be less dependent on their structures, which would be reflected by the relatively stable CD rate constants.

The CD change thus depends on two steps: one for tertiary structure change, to lower the barrier to unfolding and helix formation, and the other for secondary structure (helix) formation afterward. In some sense, the latter part depends primarily on the βLG itself, while the former is dependent on the lipid as well. Therefore, the overall CD rate constants depend not only on βLG but also on the faster fluorescence rate constants. Thus, if the k_1 primary fluorescence rate constants are fast, the CD rate constants are also going to be somewhat faster, and vice versa. However, the slower (k_2) fluorescence rate seems uncorrelated to the CD rate, suggesting these to be uncoupled processes, yet still independent of lipid concentration to some degree. This second, slower, fluorescence change reflects protection of the Trp from solvation, which could be insertion in the membrane or being fixed on the surface. Consequently, depending on the lipid permeability, the ordering of helix formation and Trp desolvation can be variable. The fact that the second rate constant for DSPG is faster than for DOPG suggests that Trp insertion or correlation to helical formation is not required.

The DMPG CD change is somewhat slower than the DOPG and DSPG ones, correlated with the slower fluorescence change

for DMPG. Dealing with the differences, we can hypothesize that DOPG's fast fluorescence rate constants are higher than for DMPG, because DOPG is more flexible than DMPG under our experimental conditions. Conversely, DSPG is studied below its transition temperature and thus is more rigid, so our results suggest that βLG may sense the charged surface created by this rigidity and more easily accommodate itself with lipid. However, this does not explain how the helix might insert into the DSPG membrane. Our earlier polarization ATR-FTIR studies in fact suggest that the helices are less inserted in DSPG (*15*).

CONCLUSION

All these observations suggest that the interaction of βLG with lipid bilayers follows a minimal model containing at least one, but probably two or more, intermediate structures:

$$\beta \xrightarrow{k_1} I_\beta \xrightarrow{k_2} I_\alpha \xrightarrow{k_3} \text{associated } \alpha \qquad (3)$$

Here we focus on what our data actually measure and assume a starting point as the monomer, so that any dimer−monomer transition in the burst phase would occur before this sequence. The model considers k_1 and k_3 as two fluorescence decay constants and k_2 as the CD decay constant. Because we consider the process to be pesudo-first-order, k_1 might vary with lipid vesicle concentration, but not significantly in the range we studied, but it does indicate that the tertiary structure of βLG becomes looser, either exposing the Trp residues or more likely reducing the level of quenching, while retaining most of its native β secondary structure that is indicated here as the I_β state. Once the tertiary structure is becomes looser, nonlocal interactions would be disrupted, letting local interactions dominate the folding process to favor helix formation. Thus, the rate (k_2) for unfolding β-sheet strands to α-helices is controlled as an intrinsic property of βLG, leading to the second intermediate state, I_α. Our previous equilibrium studies have shown that βLG finally inserts into the lipid vesicle bilayer and its helical segments are partially located in the hydrophobic part of the lipid vesicles. This process is indicated by the second fluorescence phase (k_3) and can be considered as the reassociation of a new secondary structure and a shielding tertiary structure within or on the lipid bilayers (*34*). Rate constants k_2 and k_3 are basically controlled by the intrinsic characteristics of βLG and thus do not vary much with lipid vesicle concentration but do depend on lipid permeability or flexibility controlling the degree of helix penetration.

ACKNOWLEDGMENT

We thank Ge Zhang and Weiying Zhu for assistance with checking some of the measurements.

SUPPORTING INFORMATION AVAILABLE

Details of the data and analyses of the lipid IR thermal behavior and the CD and fluorescence rate constant determinations for different runs. This material is available free of charge via the Internet at http://pubs.acs.org.

REFERENCES

1. Sawyer, L., and Kontopidis, G. (2000) The core lipocalin, bovine β-lactoglobulin. *Biochim. Biophys. Acta 1382*, 136–148.
2. Qin, B. Y., Bewley, M. C., Creamer, L. K., Baker, H. M., Baker, E. N., and Jameson, G. B. (1998) Structural basis of the Tanford transition of bovine β-lactoglobulin. *Biochemistry 37*, 14014–14023.
3. Wu, S., Perez, M. D., Puyol, P., and Sawyer, L. (1999) β-Lactoglobulin binds palmitate within its central cavity. *J. Biol. Chem. 274*, 170–174.
4. Fugate, R. D., and Song, P. S. (1980) Spectroscopic characterization of β-lactoglobulin-retinol complex. *Biochim. Biophys. Acta 625*, 28–42.
5. Molinari, H., Ragona, L., Varani, L., Musco, G., Consonni, R., Zetta, L., and Monaco, H. L. (1996) Partially folded structure of monomeric bovine β-lactoglobulin. *FEBS Lett. 381*, 237–243.
6. Townend, R., and Timasheff, S. N. (1957) The molecular weight of β-lactoglobulin. *J. Am. Chem. Soc. 79*, 3613–3614.
7. Hirota, N., Mizuno, K., and Goto, Y. (1997) Cooperative α-helix formation of β-lactoglobulin and melittin induced by hexafluoroisopropanol. *Protein Sci. 6*, 416–421.
8. Mendieta, J., Folque, H., and Tauler, R. (1999) Two-phase induction of the nonnative α-helical form of β-lactoglobulin in the presence of trifluoroethanol. *Biophys. J. 76*, 451–457.
9. Beringhelli, T., Eberini, I., Galliano, M., Pedoto, A., Perduca, M., Sportiello, A., Fontana, E., Monaco, H. L., and Gianazza, E. (2002) pH and ionic strength dependence of protein (un)folding and ligand binding to bovine β-lactoglobulin A and B. *Biochemistry 41*, 15415–15422.
10. Andrade, S. M., Carvalho, T. I., Viseu, M. I., and Costa, S. M. B. (2004) Conformational changes of β-lactoglobulin in sodium bis-(2-ethylhexyl)sulfosuccinate reverse micelles: A fluorescence and CD study. *Eur. J. Biochem. 271*, 734–744.
11. Hamada, D., Segawa, S., and Goto, Y. (1996) Non-native α-helical intermediate in the refolding of β-lactoglobulin, a predominantly β-sheet protein. *Nat. Struct. Biol. 3*, 868–873.
12. Kuwajima, K., Yamaya, H., Miwa, S., Sugai, S., and Nagamura, T. (1987) Rapid formation of secondary structure framework in protein folding studied by stopped-flow dichroism. *FEBS Lett. 221*, 115–118.
13. Arai, M., and Kuwajima, K. (1996) Rapid formation of a molten globule intermediate in refolding of α-lactalbumin. *Folding Des. 1*, 275–287.
14. Zhang, X., and Keiderling, T. A. (2006) Lipid-induced conformational transitions of β-lactoglobulin. *Biochemistry 45*, 8444–8452.
15. Zhang, X., Ge, N., and Keiderling, T. A. (2007) Electrostatic and hydrophobic interactions governing the interaction and binding of β-lactoglobulin to membranes. *Biochemistry 46*, 5252–5260.
16. Ryoichi, K., Takeshi, M., and Makoto, Y. (2000) Oxidative refolding of lysozyme assisted by negatively charged liposomes: Relationship with lysozyme-mediated fusion of liposomes. *J. Biosci. Bioeng. 90*, 14–19.
17. Matsuzaki, K., Harada, M., Handa, T., Funakoshi, S., Fujii, N., Yajima, H., and Miyajima, K. (1989) Magainin 1-induced leakage of entrapped calcein out of negatively charged lipid vesicles. *Biochim. Biophys. Acta 981*, 130–134.
18. Toni, B., Martine, M., Julie, G., and Michel, L. (1997) Melittin-induced leakage from phosphatidylcholine vesicles is modulated by cholesterol: A property used for membrane targeting. *Eur. Biophys. J. 25*, 201–210.
19. Xu, Q., and Keiderling, T. A. (2004) Effect of sodium dodecyl sulfate on folding and thermal stability of acid-denatured cytochrome c: A spectroscopic approach. *Protein Sci. 13*, 2949–2959.
20. Xu, Q., and Keiderling, T. A. (2005) Trifluoroethanol-induced Unfolding of Concanavalin A: Equilibrium and Time-resolved Optical Spectroscopical Studies. *J. Mol. Biol. 44*, 7976–7987.
21. Huang, R., Setnicka, V., Etienne, M. A., Kim, J., Kubelka, J., Hammer, R. P., and Keiderling, T. A. (2007) Cross-strand coupling of a β-hairpin peptide stabilized with an Aib-Gly turn studied using isotope-edited IR spectroscopy. *J. Am. Chem. Soc. 129*, 13592–13603.
22. Huang, R., Wu, L., McElheny, D., Bour, P., Roy, A., and Keiderling, T. A. (2009) Cross-strand coupling and site-specific unfolding thermodynamics of a trpzip β-hairpin peptide using ^{13}C isotopic labeling and IR spectroscopy. *J. Phys. Chem. B 113*, 5661–5674.
23. Anderson, R., and Davis, S. (1982) An organic phosphorus assay which avoids the use of hazardous percloric acid. *Clin. Chim. Acta 121*, 111–116.
24. Kim, M., Lee, H. J., Lee, I., Kim, I., Lim, S., Cho, H., and Kim, J. (2008) Preparation of pH-Sensitive, Long-Circulating and EGFR-Targeted Immunoliposomes. *Arch. Pharm. Res. 31*, 539–546.
25. Xu, Q., and Keiderling, T. A. (2006) Stopped-flow kinetic studies of the interaction of surfactant, sodium dodecyl sulfate, with acid-denatured cytochrome c. *Proteins: Struct., Funct., Bioinf. 63*, 571–580.
26. Marsh, D. (1974) An interaction spin label study of lateral expansion in diphalmitoyllecithin-cholesterol bilayers. *Biochim. Biophys. Acta 363*, 373–386.
27. Garidel, P., Forster, G., Richter, W., Kunst, B. H., Rapp, G., and Blume, A. (2000) 1,2-Dimyristoyl-sn-glycero-3-phophoglycerol (DMPG) divalent cation complexes: An X-ray scattering and freeze-fracture electron microscopy study. *Phys. Chem. Chem. Phys. 2*, 4537–4544.

28. Cho, Y., Batt, C. A., and Sawyer, L. (1994) Probing the Retinol-binding Site of Bovine β-lactoglobulin. *J. Biol. Chem. 269*, 11102–11107.
29. Fidorra, M., Heimburg, T., and Seeger, H. M. (2009) Melting of individual lipid components in binary lipid mixtures studied by FTIR spectroscopy, DSC and Monte Carlo simulations. *Biochim. Biophys. Acta 1788*, 600–607.
30. Kobayashi, T., Ikeguchi, M., and Sugai, S. (2000) Molten globule structure of equine β-lactoglobulin probed by hydrogen exchange. *J. Mol. Biol. 299*, 757–770.
31. Forge, V., Hoshino, M., Kuwata, K., Arai, M., Kuwajima, K., Batt, C. A., and Goto, Y. (2000) Is Folding of β-lactoglobulin Non-hierarchic? Intermediate with Native-like β-sheet and Non-native α-helix. *J. Mol. Biol. 296*, 1039–1051.
32. Kuwata, K., Shastry, R., Cheng, M., Hoshino, M., Batt, C. A., and Goto, Y. (2001) Structural and kinetic characterization of early folding events in β-lactoglobulin. *Nat. Struct. Biol. 8*, 151–155.
33. Viseu, M. I., Melo, E. P., Carvalho, T. I., Correia, R. F., and Costa, S. M. B. (2007) Unfolding kinetics of β-lactoglobulin induced by surfactant and denaturant: A stopped-flow/fluorescence study. *Biophys. J. 93*, 3601–3612.
34. Ladokhin, A. S., and White, S. H. (1999) Folding of Amphipathic Helices on Membranes: Energetics of Helix Formation by Melittin. *J. Mol. Biol. 285*, 1363–1369.